Mathematical Models of Stresses in Materials

Mathematical Models of Stresses in Materials

By

Ladislav Ceniga

Cambridge
Scholars
Publishing

Mathematical Models of Stresses in Materials

By Ladislav Ceniga

This book first published 2025

Cambridge Scholars Publishing

Lady Stephenson Library, Newcastle upon Tyne, NE6 2PA, UK

British Library Cataloguing in Publication Data
A catalogue record for this book is available from the British Library

ISBN: 978-1-0364-5100-4
ISBN (Ebook): 978-1-0364-5101-1

This monograph is dedicated with love to
my dearest parents and grandparents.

CONTENTS

INTRODUCTION

This monograph[1,2] presents original mathematical models of

- thermal and phase-transformation stresses, which originate in matrix-inclusion composites during a cooling process,
- material micro- strengthening and macro-strengthening, which is induced by these stresses,
- intercrystalline and transcrystalline crack formation, including mathematical definitions of critical limit states with respect to the material crack formation, which is induced by these stresses.

The material strengthening and the limit states represent important phenomena in material science and engineering.

The stresses are determined for a multi-inclusion-matrix model system with isotropic ellipsoidal inclusions with the inter-inclusion distance d, which are periodically distributed in an isotropic matrix. This model system corresponds to real two-component materials, which consist of

- isotropic ellipsoidal precipitates, distributed in isotropic crystal-line grains (e.g., matrix-precipitate composites),
- two types of isotropic crystalline grains with different material properties (e.g., dual-phase steel).

The thermal stresses are a consequence of different thermal expansion coefficients of the matrix and ellipsoidal inclusions. The phase-transfor-

---

[1] This monograph was reviewed by the following reviewers:
Assoc. Prof. Ing. Robert Bidulsky, PhD., visiting professor, Politecnico di Torino, Torino, Italy.
Prof.Ing. Daniel Kottfer, PhD., Alexander Dubcek University of Trencin, Faculty of Special Technology, Department of Mechanical Engineering, Trencin, Slovak Republic.

[2] This monograph was supported by the Slovak scientific grant agency VEGA 2/0069/24.

mation stresses are a consequence of a different dimension of a cubic crystalline lattice, which is transformed in the inclusion and/or matrix.

Mathematical and computational models of phenomena in infinite periodic matrix-inclusion model systems are determined within identical suitable cells, and each cell contains a central component (e.g., an inclusion, a crystalline grain, a pore). Due to this infinity and periodicity, the models, which are determined for a certain cell, are valid for any cell. Infinite matrixes are used due to simplicity of mathematical solutions for material components (e.g., precipitates, pores). The material components are small in comparison with macroscopic material samples or macroscopic structu-ral elements, and then the solutions are acceptable in spite of this simplifi-cation (Mura, 1987, 31-32).

The mathematical models results from fundamental equations of mechanics of a solid continuum, with respect to its shape, loading, mechanical constraints and the principle of minimum potential energy.

The infinite multi-inclusion-matrix model system is imaginarily divi-ded into cubic cells with the dimension d and with a central ellipsoidal inclusion, and the stresses are determined within the cubic cell. Mathematical solutions for this multi-inclusion-matrix model system correspond to real composites, in contrast to

- the simple one-inclusion mathematical model in (Selsing, 1961, 419-419), determined for a simple one-inclusion-matrix model system,
- the simple multi-inclusion mathematical model in (Mizutani, 1996, 483-494), determined for physically unacceptable mechani-cal constraints due to unsuitable cells of a multi-inclusion-matrix system.

Different mathematical procedures, which are applied to the fundame-ntal equations (Cauchy's and equilibrium equations, Hooke's law), result in different mathematical solutions for the stresses in the matrix and ellipsoidal inclusion. Finally, such a combination of the different mathematical solutions for the matrix and the ellipsoidal inclusion is considered to exhibit minimum potential energy.

The mathematical models are determined by standard procedures of mechanics of a solid continuum, which include definitions of

- such a multi-inclusion-matrix model system and a coordinate sys-tem, which correspond to real matrix-inclusion composite ma-terials,

- reasons of the thermal and phase-transformation stresses,
- the fundamental equations, which result in a system of differen-tial equations,
- elastic energy density and elastic energy of the model system,
- mechanical constraints, i.e., mathematical boundary conditions, for the matrix and ellipsoidal inclusion,
- different mathematical procedures, which are applied to the sys-tem of the differential equations,
- final formulae for the thermal and phase-transformation stresses, strains, elastic energy density and elastic energy,
- final formulae for the material micro-/macro-strengthening in the matrix and ellipsoidal inclusion,
- mathematical procedures to determine such critical dimensions of the ellipsoidal inclusion, which are reason of a crack in the ma-trix,
- mathematical procedures to determine dimensions of the matrix crack.

In contrast to author's mathematical models (Ceniga, 2008, 10-11; 2007, 9-12) for composites with inclusions of an ideal spherical shape, the mathematical models in this monograph, which are determined for composites with ellipsoidal inclusions, represent a more realistic description of the stress-strain state in real matrix-inclusion composite materials.

The mathematical results in this monograph are then applicable within

- basic research (mechanics of a solid continuum, theoretical physics, material science),
- the engineering practice, i.e., material technology,
- as well as within university undergraduate and postgraduate cour-ses, as a textbook on analytical material mechanics.

With regard to the basic research, the results of this monograph can be incor-porated to mathematical models, which defines the disturbance of an ap--plied stress field around inclusions in a solid continuum (Eshelby, 1957, 376-396), as well as into mathematical, computational and experimental models of overall materials stresses, overall material strengthening, inter-actions of energy barriers with dislocations and domain walls, etc.

The mathematical models include microstructural parameters of a real matrix-inclusion composite (the inclusion dimensions a_{1IN}, a_{2IN}, a_{3IN}, the inclusion volume fraction v_{IN}, the inter-inclusion distance d), and are applicable to composites with ellipsoidal inclusions of different morpholo-

gy, i.e., $a_{1IN} \approx a_{2IN} \approx a_{3IN}$ (dual-phase steel), $a_{1IN} >> a_{2IN} \approx a_{3IN}$ (martensitic steel).

In case of real two-component materials (the engineering practice), material scientists and engineers can determine such numerical values of the microstructural parameters,

- which result in maximum values of the material micro-and ma-cro-strengthening,
- which define the limit states (i.e., critical states) with respect to the intercrystalline or transcrystalline crack formation in the ma-trix and the ellipsoidal inclusion.

Consequently, the material scientists and engineers can develop sui-table technological processes, which result in such microstructural para-meters to obtain maximum strengthening, and to avoid the crack forma-tion.

This numerical determination, performed by suitable programming languages, result from the mathematical procedure in Appendix.

With respect to the university courses, the fundamental equations of mechanics of a solid continuum, along with the mathematical procedures, are explained and determined in detail. As a textbook on analytical material mechanics, this monograph is then suitable for non-specialists in mechanics of a solid continuum. Finally, Appendix presents such mathematical topics, which are required to perform the mathematical procedures in this monograph.

Ladislav Ceniga
Institute of Materials Research
Slovak Academy of Sciences
Kosice, Slovak Republic

CHAPTER 1

MODEL MATERIAL SYSTEM

1.1 Matrix-Inclusion System

Figure 1.1 shows the model material system, which consists of an infi-nite matrix and periodically distributed ellipsoidal inclusions with the dimensions a_{1IN}, a_{2IN}, a_{3IN} along the axes x_1, x_2, x_3 of the Cartesian system ($Ox_1x_2x_3$), respectively, and with the inter-inclusion distance d along x_1, x_2, x_3. The point O is a centre of the ellipsoidal inclusion.

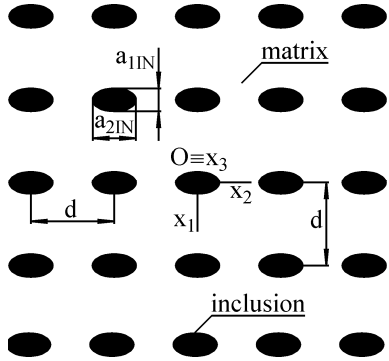

Figure 1.1. The matrix-inclusion system with infinite matrix and periodi-cally distributed ellipsoidal inclusions: the dimensions a_{1IN}, a_{2IN}, a_{3IN} along the axes x_1, x_2, x_3 of the Cartesian system ($Ox_1x_2x_3$), respectively; the inter-inclusion distance d along the axes x_1, x_2, x_3; the inclusion centre O.

The mathematical models of the thermal and phase-transformation stresses are determined in the cubic cell with the dimension d and with a central ellipsoidal inclusion (see Figure 1.2). With regard to the volume $V_{IN} = 4\pi a_{1IN} a_{2IN} a_{3IN}$ and $V_C = d^3$ of the ellipsoidal inclusion and the cubic cell, the inclusion volume fraction v_{IN} and the inter-inclusion distance d have the forms

$$v_{IN} = \frac{V_{IN}}{V_C} = \frac{4\pi\, a_{1IN}\, a_{2IN}\, a_{3IN}}{3d^3} \in \left(0, \frac{\pi}{6}\right),$$

$$d = \left(\frac{4\pi\, a_{1IN}\, a_{2IN}\, a_{3IN}}{3 v_{IN}}\right)^{1/3}, \tag{1.1}$$

where $v_{INmax} = \pi / 6$ is given by the condition $a_i \rightarrow$ d/2 (i = 1,2,3). The inter-inclusion distance $d = d(a_{1IN}, a_{2IN}, a_{3IN}, v_{IN})$ is included within the mechanical constraints (see Equations (1.15), (4.1)-(4.5)), and the stresses are a function of the microstructural parameters a_{1IN}, a_{2IN}, a_{3IN}, v_{IN}, d.

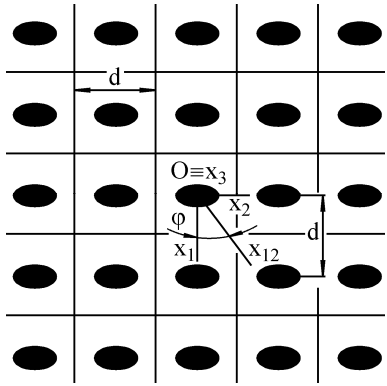

Figure 1.2. The cubic cells with the dimension d and with the plane x_1x_2, where O is a centre of the ellipsoidal inclusions, and $x_{12} \subset x_1x_2$, $x_{12}x_3 \subset x_1x_2$.

This model system corresponds to real two-component materials, which consist of

- isotropic ellipsoidal precipitates, distributed in isotropic crystal-line grains, e.g., matrix-precipitate composites,
- two types of isotropic crystalline grains with different material properties, e.g., dual-phase steel with the grains A and B.

Consequently, the ellipsoidal precipitates and the crystalline grains are considered to represent the ellipsoidal inclusion and the matrix of the model matrix-inclusion system.

Similarly, let the crystal grains A and B be characterized by the volume fraction v_A and v_B, respectively, where $v_A+v_B=1$. If $v_A<v_B$, then the grains A and B are considered to represent the ellipsoidal inclusion and the matrix, respectively. If $v_A>v_B$, then the grains A and B are considered to represent the matrix and the ellipsoidal inclusion, respectively. If $v_A=v_B$, then the following energy analysis is required to be consi-dered.

Let the grains A and B be considered to represent the ellipsoidal inclu-sion and the matrix with the elastic energy W_{INA} and W_{MB}, which is accu-mulated in the ellipsoidal inclusion and the cell matrix (see Equation (2.30)), respectively.

Let the grains A and B be considered to represent the matrix and the ellipsoidal inclusion with the elastic energy W_{MA} and W_{INB}, which is accumulated in the cell matrix and the ellipsoidal inclusion (see Equation (2.30)), respectively.

If $W_{INA} + W_{MB} < W_{MA} + W_{INB}$, then the grains A and B are considered to represent the ellipsoidal inclusion and the matrix, respectively. If $W_{INA} + W_{MB} > W_{MA} + W_{INB}$, the grains A and B are considered to represent the matrix and the ellipsoidal inclusion, respectively.

Mathematical and computational models of phenomena in infinite periodic matrix-inclusion model systems are determined within identical suitable cells. Due to this infinity and periodicity, the mathematical models of the thermal and phase-transformation stresses in the multi-inclusion model system in Figures 1.1, 1.2, which are determined for a certain cell, are valid for any cell. In general, infinite matrixes are used due to simplicity of mathematical solutions for material components (e.g., precipitates, crystalline grains, pores). Such mathematical solutions are assumed to exhibit sufficient accurancy with respect to material components (e.g., precipitates, crystalline grains, pores), which are small in comparison with macroscopic material samples and macroscopic structural elements. Finally, the mathematical solutions are acceptable in spite of this simplification (Mura, 1987, 31-32).

1.2 Coordinate System

The ellipse E with the dimensions a, b along the axes x, y of the Carte-sian system (Oxy), respectively, is described by the function (Rektorys, 1973, 147)

$$\left(\frac{x}{a}\right)^2+\left(\frac{y}{b}\right)^2=1,\quad x=a\cos\alpha,\quad x=b\sin\alpha\,, \tag{1.2}$$

where x, y are coordinates of any point P of the ellipse E. The normal n at the point P has the form (Rektorys, 1973, 148)

$$\frac{\partial x}{\partial\alpha}\left(x-a\cos\alpha\right)+\frac{\partial y}{\partial\alpha}\left(x-b\sin\alpha\right)=0\,. \tag{1.3}$$

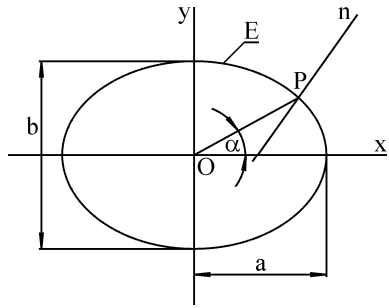

Figure 1.3. The ellipse E with the dimensions a, b along the axes x, y of the Cartesian system (Oxy), respectively, and the P related to the angle α.

With regard to Equations (1.2), (1.3), we get

$$y=\frac{1}{b}\left[x\,a\tan\alpha-\left(a^2-b^2\right)\sin\alpha\right]. \tag{1.4}$$

The stresses are determined by the spherical coordinates (x_n,φ,ν), where $x_n=|P_{12}P|$, $P_{12}\subset x_{12}$ (see Figure 1.4). Equations (1.12), (1.13) define a fuction $\theta=f(\nu)$ for the angles $\theta,\nu\in\langle 0,\pi/2\rangle$. The model system is symmetric (see Figure 1.1, 1.2), and the stresses are sufficient to be determined within the interval $\varphi,\nu\in\langle 0,\pi/2\rangle$. Figure 1.4 shows the ellipsoidal inclusion for φ, $\nu\in\langle 0,\pi/2\rangle$, where $a_{1IN}=O1$, $a_{2IN}=O2$, $a_{3IN}=O3$. With regard to Equation (1.2), any point of the ellipse E_{12} in the plane x_1x_2 has the coordinates

$$x_1=a_{1IN}\cos\varphi,\quad x_2=a_{2IN}\sin\varphi,\quad \varphi\in\left\langle 0,\frac{\pi}{2}\right\rangle. \tag{1.5}$$

The point P of the ellipse E_{123} in $x_{12}x_3$ is described by the coordinates

$$x_{12P} = a_{12}\sin\nu, \quad x_{3P} = a_3\cos\nu,$$
$$a_{12} = O4 = \sqrt{a_{1IN}^2\cos^2\varphi + a_{2IN}^2\sin^2\varphi}, \quad \varphi,\nu \in \left\langle 0, \frac{\pi}{2} \right\rangle. \tag{1.6}$$

where $(Px_nx_\varphi x_\theta)$ is a Cartesian system at the point P; the axes x_n and x_θ represents a normal and a tangent of the ellipse E_{123} at the point P, respectively; and $x_{12}x_3 \perp x_1x_2$, $x_{12} \subset x_1x_2$, $x_\varphi \perp x_{12}$.

Figure 1.5 shows the cross section $O567$ of the cubic cell in the plane $x_{12}x_3$ (see Figures 1.2, 1.4). The angle $\nu \in \langle 0, \pi/2 \rangle$ defines a position of the point P with the Cartesian system $(Px_nx_\varphi x_\theta)$ (see Figure 1.4) for $\nu = \nu_0$ (see Figure 1.5a), $\nu \in (0, \nu_0\rangle$ (see Figure 1.5b), $\nu \in \langle \nu_0, \pi/2\rangle$ (see Figure 1.5c). The points P_1, P_2 represent intersections of the normal x_n with O567.

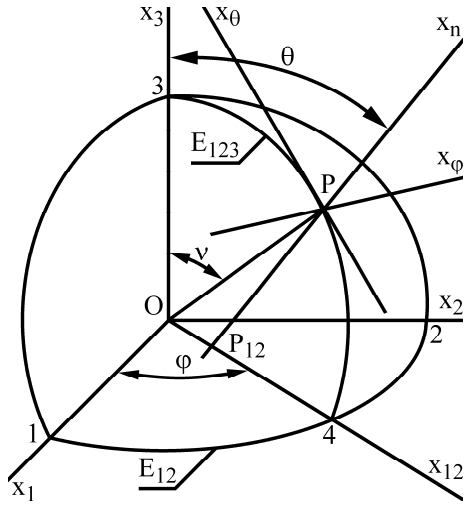

Figure 1.4. The inclusion with the centre O and with the dimensions $a_{1IN} = O1$, $a_{2IN} = O2$, $a_{3IN} = O1$ along the axes x_1, x_2, x_3, respectively. The ellipses E_{12}, E_{123} in the planes x_1x_2, $x_{12}x_3$ (see Figure 1.2) are given by Equations (1.5), (1.6), respectively, where $x_{12}x_3 \perp x_1x_2$, $x_{12} \subset x_1x_2$, $x_\varphi \perp x_{12}$. The point P on the inclusion surface is defined by φ, $\nu \in \langle 0, \pi/2\rangle$, and $(Px_nx_\varphi x_\theta)$ is a Cartesian system at the point P, where $P \subset E_{123}$. The axes x_n and x_θ represents a normal and a tangent of the ellipse E_{123} at the point P, where $x_n = |P_{12}P|$, $P_{12} \subset x_{12}$. The function $\theta = f(\nu)$ is given by Equations (1.12), (1.13).

With regard to Equation (1.4), the normal x_n at the point P of the ellipse E_{123} in the plane $x_{12}x_3$ is derived as

$$x_3 = \frac{\cos\nu}{a_3}\left(\frac{a_{12}\,x_{12}}{\sin\nu} + a_3^2 - a_{12}^2\right), \quad \nu \in \left\langle 0, \frac{\pi}{2}\right\rangle . \tag{1.7}$$

With regard to Equation (1.7), the coordinates x_{121}, x_{31} of the point P_1 is derived as

$$x_{121} = \frac{\left(a_{12}^2 - a_3^2\right)\sin\nu}{a_{12}}, \quad x_{31} = 0, \quad \nu \in \left\langle 0, \frac{\pi}{2}\right\rangle , \tag{1.8}$$

The coordinates x_{122}, x_{32} of the point P_2 in Figure 1.5b for $\nu \in (0, \nu_0\rangle$ are derived as

$$x_{122} = \frac{\sin\nu}{a_{12}}\left(\frac{d\cos\nu}{2a_3} + a_{12}^2 - a_3^2\right), \quad x_{32} = \frac{d}{2} \quad \nu \in \left\langle 0, \nu_0\right\rangle . \tag{1.9}$$

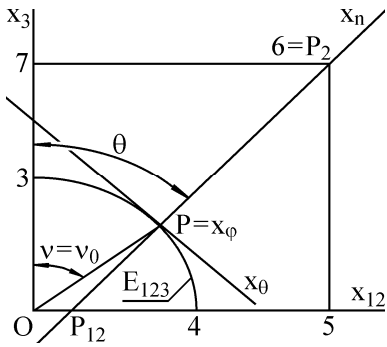

(a)

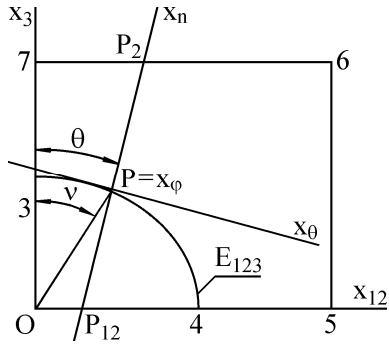

(b)

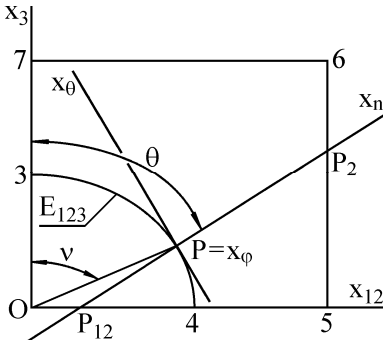

(c)

Figure 1.5. The angle $\nu \in \langle 0, \pi/2 \rangle$ defines a position of the point P with the Cartesian system $(Px_n x_\varphi x_\theta)$ (see Figure 1.4) for (a) $\nu \in \langle 0, \pi/2 \rangle$, (b) $\nu \in (0, \nu_0 \rangle$ (c) $\nu \in \langle \nu_0, \pi/2 \rangle$, where ν_0 is given by Equation (1.7). The points P_{12} (see Figure 1.4), P_2 represent intersections of the normal x_n with *O567*, where *O567* is a cross section of the cubic cell in the plane $x_{12}x_3$ (see Figures 1.2, 1.4). The angle $\theta = \angle(x_n, x_3)$ is given by Equation (1.11).

The coordinates x_{122}, x_{32} of the point P_2 in Figure 1.5c for $\nu \in \langle \nu_0, \pi/2 \rangle$ have the forms

$$x_{122} = \frac{d}{2c_\varphi \sin\nu},$$

$$c_\varphi = \cos\varphi, \quad \varphi \in \left\langle 0, \frac{\pi}{4} \right\rangle; \quad c_\varphi = \sin\varphi, \quad \varphi \in \left\langle \frac{\pi}{4}, \frac{\pi}{2} \right\rangle$$

$$x_{32} = \frac{\cos\nu}{a_3}\left[\frac{a_{12}\, d}{2 f(\varphi)\sin\nu} + a_3^2 - a_{12}^2\right], \quad \nu \in \left\langle \nu_0, \frac{\pi}{2} \right\rangle. \tag{1.10}$$

The coordinate x_{122} of the point P_2 in Figure 1.5a for $\nu \in (0, \nu_0 \rangle$ is given by Equation (1.10), where $x_{32} = d/2$. With regard to Equation (1.7), the angle ν_0 represents a root of the following equation

$$\frac{\cos\nu_0}{a_3}\left[\frac{a_{12}\, d}{2f(\varphi)\sin\nu_0} + a_3^2 - a_{12}^2\right] - \frac{d}{2} = 0,$$

$$f(\varphi) = \cos\varphi, \quad \varphi \in \left\langle 0, \frac{\pi}{4} \right\rangle; \quad f(\varphi) = \sin\varphi, \quad \varphi \in \left\langle \frac{\pi}{4}, \frac{\pi}{2} \right\rangle, \tag{1.11}$$

and this root is determined by a numerical method. The angle $\theta = \angle(x_n, x_3)$ has the form

$$\cos\theta = \frac{x_{3P}}{\sqrt{\left(x_{12P} - x_{121}\right)^2 + x_{3P}^2}} = \frac{1}{\sqrt{1 + \left(\dfrac{a_3 \tan\nu}{a_{12}}\right)^2}},$$

$$\sin\theta = \frac{1}{\sqrt{1 + \left(\dfrac{a_3 \cot\nu}{a_{12}}\right)^2}}. \tag{1.12}$$

and then we get

$$\sin\theta\, d\theta = \Omega\, d\nu, \quad \Omega = \frac{1}{\sqrt{\left(\dfrac{a_3}{a_{12}}\right)^2 + \cot^2\nu}\left[\left(\dfrac{a_3}{a_{12}}\right)^2 + \cot^2\nu\right]\sin^2\nu},$$

$$\frac{\partial}{\partial\theta} = \left(\frac{\partial\theta}{\partial\nu}\right)^{-1}\frac{\partial}{\partial\nu} = \Theta\frac{\partial}{\partial\nu}, \quad \Theta = \frac{a_{12}}{a_3}\left[\left(\frac{a_3 \sin\nu}{a_{12}}\right)^2 + \cos^2\nu\right]. \tag{1.13}$$

The model system in Figure 1.1 is symmetric. Due to this symmetry, any point P on the matrix-inclusion boundary exhibit the normal displace-ment u_n along the axis x_n. Consequently, any point P of the normal x_n exhi-bits u_n, and then we get $u_\varphi = u_\theta$, where u_φ, u_θ are displacement along the axes x_φ, x_θ, respectively.

The stresses are determined along the axes x_n, x_φ, x_θ of the Cartesian system ($P\ x_n\ x_\varphi\ x_\theta$), and represent functions of the spherical coordinates (x_n, φ, θ) for φ, $\theta \in \langle 0, \pi/2\rangle$. The intervals $x_n \in \langle 0, x_{IN}\rangle$ and $x_n \in \langle x_{IN}, x_M\rangle$ are related to the ellipsoidal inclusion and the cell matrix, where $P = P_1$, $P \subset E_{123}$ and $P = P_2$ for $x_n = 0$, $x_n = x_{IN}$ and $x_n = x_M$ (see Figure 1.5), respectively. Finally, we get

$$x_{IN} = P_1P = \sqrt{\left(x_{12P} - x_{121}\right)^2 + x_{3P}^2} = a_3\sqrt{\left(\frac{a_3 \sin\nu}{a_{12}}\right)^2 + \cos^2\nu},$$

$$x_M = PP_2 = \sqrt{\left(x_{122} - x_{12P}\right)^2 + \left(x_{32} - x_{3P}\right)^2}$$

$$= \sqrt{\left(\frac{\sin\nu}{a_{12}}\right)^2\left(\frac{d\cos\nu}{2a_3} - a_3^2\right)^2 + \left(\frac{a_{12}\cos\nu}{a_3}\right)^2\left[\frac{d}{2f(\varphi)\sin\nu} - a_{12}\right]^2} \,. \tag{1.15}$$

CHAPTER 2

FUNDAMENTAL EQUATIONS

Fundamental equations of mechanics of a solid continuum are repre-sented by Cauchy's and equilibrium equations, along with Hooke's law (see Section 2.1-2.3), which result in a system of differential equations (see Section 2.4). Due to different mathematical solutions of this systems, which are determined by different mathematical procedures (see Sections 5.1,6.1,7.1,8.1), the analysis of elastic energy density is considered (see Section 2.8).

2.1 Cauchy's Equations

Cauchy's equations define relationships between strains and displacements, and are determined for a suitable infinitesimal part of the model system with respect to a coordinate system (see Figures 1.1, 1.2).

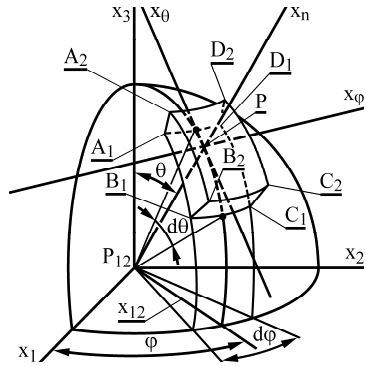

Figure 2.1. The infinitesimal spherical cap at the point P with the surface $S_1 = A_1B_1C_1D_1$ and $S_2 = A_2B_2C_2D_2$ for $x_n = P_{12}P$ (see Figure 1.4) and x_n+dx_n, respectively, where $A_1A_2=B_1B_2=C_1C_2=D_1D_2=dx_n$, $A_1D_1=B_1C_1= x_n\times d\varphi$, $A_1B_1=C_1D_1=x_n\times d\theta$, $A_2D_2=B_2C_2=(x_n+dx_n)\times d\varphi$, $A_2B_2=C_2D_2=(x_n+dx_n) \times d\theta$. The axes x_n and x_φ, x_θ represent normal and tangential directions (see Figure 1.4), respetively.

Due to the spherical coordinates (r,φ,ν) (see Figure 1.4), the infinitesimal part at the point P is represented by the infinitesimal spheri-cal cap with the dimension $A_1A_2=B_1B_2=C_1C_2=D_1D_2=dx_n$ along the axis x_n, and with the dimensions $A_1A_2=B_1B_2=C_1C_2=D_1D_2=dx_n$, $A_1D_1=B_1C_1=x_n\times d\varphi$, $A_1B_1=C_1D_1=x_n\times d\theta$ and $A_2D_2=B_2C_2=(x_n+dx_n)\times d\varphi$, $A_2B_2= C_2D_2=(x_n+dx_n)\times d\theta$ along the axes x_φ, x_θ for $x_n = P_{12}P$ (see Figure 1.4) and x_n+dx_n, respectively. The axes x_n and x_φ, x_θ represent normal and tangential directions (see Figure 1.4), respetively.

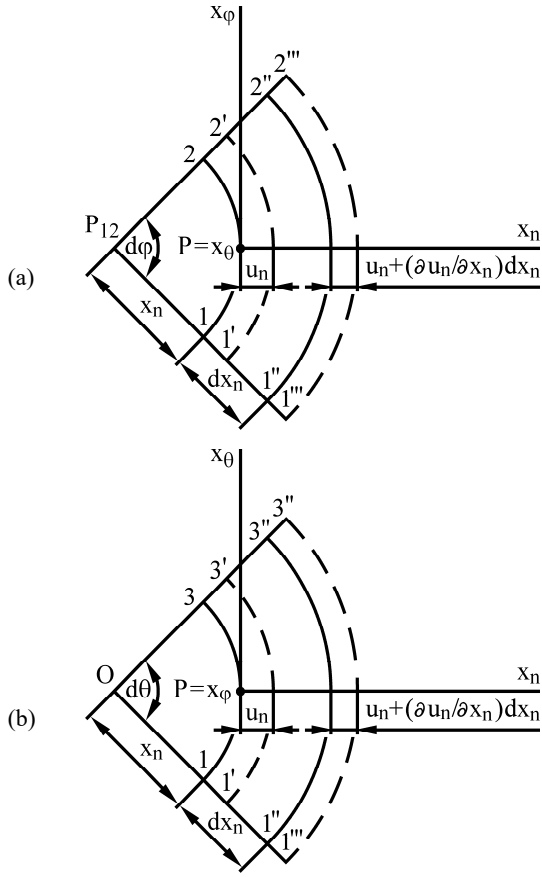

Figure 2.2. The normal displacement u_n and $u_n+(\partial u_n/\partial x_n)\ dx_n$ of the infini-tesimal spherical cap at the point P for $x_n = P_{12}P$ and x_n+dx_n in the plane (a) x_nx_φ, (b) $x_n\ x_\theta$ (see Figures 1.4, 2.1), respectively.

As analysed in Chapter 1, any point P of the normal x_n (see Figure 1.4) exhibits the normal displacement u_n along the normal x_n, and then we get $u_\varphi = u_\theta$, where u_φ, u_θ are displacement along the axes x_φ, x_θ, respectively. The stresses are determined along the axes x_n, x_φ, x_θ of the Cartesian system ($Px_nx_\varphi x_\theta$).

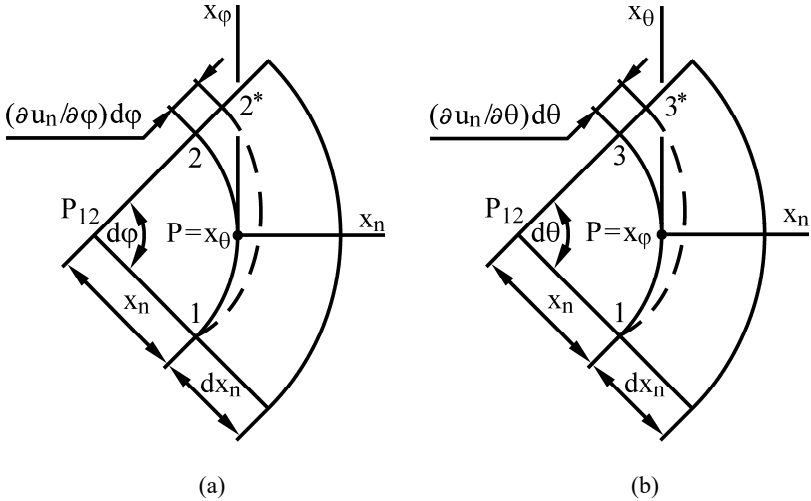

Figure 2.3. The normal displacement $u_n = u_n(\varphi,\theta)$ of the infinitesimal sphe-rical cap at the point P in the plane (a) $x_n x_\varphi$, (b) $x_n x_\theta$ (see Figures 1.4, 2.1).

With regard to Figure 2.2, the normal strain ε_n along the axis x_n, and the tangential strains ε_φ, ε_θ along the axes x_φ, x_θ, respectively, are derived as (Ceniga, 2007, 35-38; Ceniga, 2008, 23-26)

$$\varepsilon_n = \frac{\left|1'''1'\right| - \left|1''1'\right|}{\left|1''1'\right|} = \frac{1}{dx_n}\left[\left(dx_n + \frac{\partial u_n}{\partial x_n}\,dx_n\right) - dx_n\right] = \frac{\partial u_n}{\partial x_n}, \qquad (2.1)$$

$$\varepsilon_\varphi = \varepsilon_\theta = \frac{\left|1'2'\right| - \left|12\right|}{\left|12\right|} = \frac{\left|1'3'\right| - \left|13\right|}{\left|13\right|}$$

$$= \frac{(u_n + x_n)\,d\varphi - x_n\,d\varphi}{x_n\,d\varphi} = \frac{(u_n + x_n)\,d\theta - x_n\,d\theta}{x_n\,d\theta} = \frac{u_n}{x_n}, \qquad (2.2)$$

where $|13| = x_n\, d\theta$, $|1'3'| = (u_n + x_n)\, d\theta$ is considered instead of $|13| = x_n \sin\theta\, d\theta$, $|1'3'| = (u_n + x_n) \sin\theta\, d\theta$ (Brdicka, 2000, 73-75), respectively. With regard to Figure 2.3, the shear strains $\varepsilon_{n\varphi}$, $\varepsilon_{n\theta}$ and $\varepsilon_{\varphi n}$, $\varepsilon_{\theta n}$ along the axes x_n and x_φ, x_θ, respectively, have the forms (Ceniga, 2007, 35-38; Ceniga, 2008, 23-26)

$$\varepsilon_{n\varphi} = \tan\left[\angle\left(|12|,\left|12^*\right|\right)\right] = \frac{1}{x_n\, d\varphi}\left(\frac{\partial u_n}{\partial \varphi}\, d\varphi\right) = \frac{1}{x_n}\frac{\partial u_n}{\partial \varphi}, \tag{2.3}$$

$$\varepsilon_{n\theta} = \tan\left[\angle\left(|13|,\left|13^*\right|\right)\right] = \frac{1}{x_n\, d\theta}\left(\frac{\partial u_n}{\partial \theta}\, d\theta\right) = \frac{1}{x_n}\frac{\partial u_n}{\partial \theta} = \frac{\Theta}{x_n}\frac{\partial u_n}{\partial \nu}, \tag{2.4}$$

where Θ is given by Equation (1.13), and $\varepsilon_{n\varphi} = \varepsilon_{\varphi n}$, $\varepsilon_{n\theta} = \varepsilon_{\theta n}$ (Brdicka, 2000, 68-71). Due to $u_\varphi = u_\theta$, we get $\varepsilon_{\varphi\theta} = \varepsilon_{\theta\varphi} = \propto (\partial u_\varphi/\partial\theta) + (\partial u_\theta/\partial\varphi) = 0$, $\varepsilon_{\varphi\theta}$ and $\varepsilon_{\theta\varphi}$ are shear strains along the axes x_φ, x_θ, respectively.

2.2 Equilibrium Equations

Mechanics of a solid continuum results from the condition of the equilibrium of forces, which acts on sides of an infinitesimal part of a solid continuum. The equilibrium equations of the forces, which act on the sides of the infinitesimal spherical cap are determined with respect to the axes x_n, x_φ, x_θ at the point P (see Figure 2.1). In case of the axis x_n (see Figure 2.4), we get (Ceniga, 2007, 35-38; Ceniga, 2008, 23-26)

$$\begin{aligned}
&\left(\sigma_n + \frac{\partial \sigma_n}{\partial x_n}\, dx_n\right)\left(x_n + dx_n\right) d\varphi \left(x_n + dx_n\right) d\theta \\
&+\left(\sigma_{n\varphi} + \frac{\partial \sigma_{n\varphi}}{\partial \varphi}\, d\varphi\right) \cos\left(\frac{d\varphi}{2}\right) x_n\, d\theta\, dx_n \\
&+\left(\sigma_{n\theta} + \frac{\partial \sigma_{n\theta}}{\partial \theta}\, d\theta\right) \cos\left(\frac{d\theta}{2}\right) x_n\, d\varphi\, dx_n \\
&-\left[\sigma_n\, x_n\, d\varphi\, x_n\, d\theta + \left(\sigma_\varphi + \frac{\partial \sigma_\varphi}{\partial \varphi}\, d\varphi\right) \sin\left(\frac{d\varphi}{2}\right) x_n\, d\theta\, dx_n\right.
\end{aligned}$$

$$+\left(\sigma_\theta+\frac{\partial\sigma_\theta}{\partial\theta}\,d\theta\right)\sin\left(\frac{d\theta}{2}\right)x_n\,d\varphi\,dx_n+\sigma_\varphi\,\sin\left(\frac{d\varphi}{2}\right)x_n\,d\theta\,dx_n$$

$$+\sigma_\theta\,\sin\left(\frac{d\theta}{2}\right)x_n\,d\varphi\,dx_n+\sigma_{n\varphi}\,\cos\left(\frac{d\varphi}{2}\right)x_n\,d\theta\,dx_n$$

$$+\sigma_{n\theta}\,\cos\left(\frac{d\theta}{2}\right)x_n\,d\varphi\,dx_n\Bigg]=0\,, \tag{2.5}$$

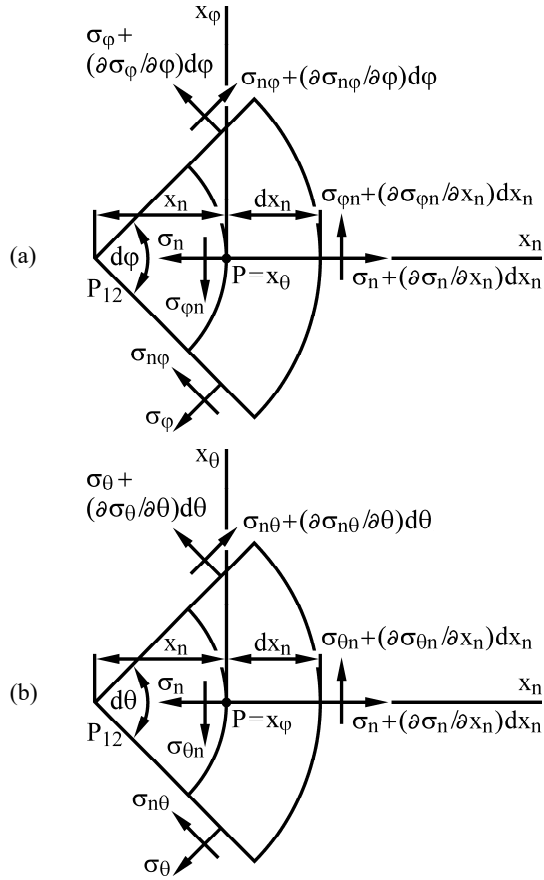

Figure 2.4. The infinitesimal spherical cap in the plane (a) $x_n x_\varphi$, (b) $x_n x_\theta$ (see Figures 1.4, 2.1). The normal stress σ_n, the tangential stresses σ_φ, σ_θ, the shear stresses $\sigma_{n\varphi} = \sigma_{\varphi n}$, $\sigma_{n\theta} = \sigma_{\theta n}$, along with changes of these stresses, acting on the sides of the infinitesimal spherical cap at the point P.

In case of the axis x_φ (see Figure 2.4), we get

$$\left(\sigma_\varphi+\frac{\partial\sigma_\varphi}{\partial\varphi}\,d\varphi\right)\cos\left(\frac{d\varphi}{2}\right)x_n\,d\theta\,dx_n$$
$$+\left(\sigma_{\varphi n}+\frac{\partial\sigma_{\varphi n}}{\partial x_n}\,dx_n\right)\left(x_n+dx_n\right)d\varphi\left(x_n+dx_n\right)d\theta$$
$$+\left(\sigma_{n\varphi}+\frac{\partial\sigma_{n\varphi}}{\partial\varphi}\,d\varphi\right)\sin\left(\frac{d\varphi}{2}\right)x_n\,d\theta\,dx_n+\sigma_{n\varphi}\sin\left(\frac{d\varphi}{2}\right)x_n\,d\theta\,dx_n$$
$$-\left(\sigma_\varphi\cos\left(\frac{d\varphi}{2}\right)x_n\,d\theta\,dx_n+\ \sigma_{\varphi n}\,x_n\,d\varphi\,x_n\,d\theta\right)=0\,, \tag{2.6}$$

In case of the axis x_θ (see Figure 2.4), we get

$$\left(\sigma_\theta+\frac{\partial\sigma_\theta}{\partial\theta}\,d\theta\right)\cos\left(\frac{d\theta}{2}\right)x_n\,d\varphi\,dx_n$$
$$+\left(\sigma_{\theta n}+\frac{\partial\sigma_{\theta n}}{\partial x_n}\,dx_n\right)\left(x_n+dx_n\right)d\varphi\left(x_n+dx_n\right)d\theta$$
$$+\left(\sigma_{n\theta}+\frac{\partial\sigma_{n\theta}}{\partial\theta}\,d\theta\right)\sin\left(\frac{d\theta}{2}\right)x_n\,d\varphi\,dx_n+\sigma_{n\theta}\sin\left(\frac{d\theta}{2}\right)x_n\,d\varphi\,dx_n$$
$$-\left(\sigma_\theta\cos\left(\frac{d\theta}{2}\right)x_n\,d\varphi\,dx_n+\ \sigma_{\theta n}\,x_n\,d\varphi\,x_n\,d\theta\right)=0\,. \tag{2.7}$$

where $|13| = x_n\,d\theta$, $|1'3'| = (u_n + x_n)\,d\theta$ is considered instead of $|13| = x_n \sin\theta\,d\theta$, $|1'3'| = (u_n + x_n)\sin\theta\,d\theta$ (Brdicka, 2000, 73-75), respectively. Due to $d\varphi \approx 0$, $d\theta \approx 0$, $dr \approx 0$, we get $\sin(d\varphi/2)\approx d\varphi/2$, $\sin(d\theta/2)\approx d\theta/2$, $\cos(d\varphi/2) = \cos(d\theta/2) \approx 1$, $(dr)^2 = (d\varphi)^2 = (d\theta)^2 = 0$ (Brdicka, 2000, 76-77). Consequently, the equilibrium equations (2.5)-(2.7) are derived as (see Equation (1.13))

$$2\sigma_n-\sigma_\varphi-\sigma_\theta+x_n\frac{\partial\sigma_n}{\partial x_n}+\frac{\partial\sigma_{n\varphi}}{\partial\varphi}+\Theta\frac{\partial\sigma_{n\theta}}{\partial\nu}=0\,, \tag{2.8}$$

$$\frac{\partial \sigma_{\varphi}}{\partial \varphi} + 3\sigma_{n\varphi} + x_n \frac{\partial \sigma_{n\varphi}}{\partial x_n} = 0\,, \tag{2.9}$$

$$\Theta \frac{\partial \sigma_{\theta}}{\partial \nu} + 3\sigma_{n\theta} + x_n \frac{\partial \sigma_{n\theta}}{\partial x_n} = 0\,, \tag{2.10}$$

where σ_{n} and σ_{φ}, σ_{θ} are normal and tangential stress along the axes x_{n} and x_{φ}, x_{θ}, respectively; $\sigma_{\mathrm{n}\varphi}$, $\sigma_{\mathrm{n}\theta}$ and $\sigma_{\varphi\mathrm{n}}$, $\sigma_{\theta\mathrm{n}}$ are shear stress along the axes x_{n} and x_{φ}, x_{θ}, respectively. Due to $\varepsilon_{\varphi\theta} = \varepsilon_{\theta\varphi}$, we get $\sigma_{\varphi\theta} = \sigma_{\theta\varphi} = 0$, where $\sigma_{\varphi\theta}$ is a shear stress.

2.3 Hooke Law

With regard to $\varepsilon_{\varphi\theta} = 0$, $\sigma_{\varphi\theta} = 0$, Hooke's law has the form (Brdicka, 2000, 60-62)

$$\varepsilon_n = s_{11}\sigma_n + s_{12}\left(\sigma_{\varphi} + \sigma_{\theta}\right), \tag{2.11}$$

$$\varepsilon_{\varphi} = s_{12}\left(\sigma_n + \sigma_{\theta}\right) + s_{11}\sigma_{\varphi}\,, \tag{2.12}$$

$$\varepsilon_{\theta} = s_{12}\left(\sigma_n + \sigma_{\varphi}\right) + s_{11}\sigma_{\theta}\,, \tag{2.13}$$

$$\varepsilon_{n\theta} = s_{44}\sigma_{n\theta}\,, \tag{2.14}$$

$$\varepsilon_{n\varphi} = s_{44}\sigma_{n\varphi}\,, \tag{2.15}$$

where s_{11}, s_{12} have the form (Brdicka, 2000, 62-63)

$$s_{11} = \frac{1}{E}, \quad s_{12} = -\frac{\mu}{E}, \quad s_{11} = \frac{2(1+\mu)}{E}\,, \tag{2.16}$$

and E, μ represent Young modulus, Poisson's ratio (Brdicka, 2000, 60-62), respectively. In case of the ellipsoidal inclusion and the matrix, we get $E = E_{\mathrm{IN}}$, $\mu = \mu_{\mathrm{IN}}$ and $E = E_{\mathrm{M}}$, $\mu = \mu_{\mathrm{M}}$, respectively. With regard to Equations (2.1)-(2.4), (2.11)-(2.15), we get (Ceniga, 2007, 22-23; Ceniga, 2008, 27-28)

$$\sigma_n = (c_1 + c_2)\frac{\partial u_n}{\partial x_n} - 2c_2\frac{u_n}{x_n}, \tag{2.17}$$

$$\sigma_\varphi = \sigma_\theta = -c_2\frac{\partial u_n}{\partial x_n} + c_1\frac{u_n}{x_n}, \tag{2.18}$$

$$\sigma_{n\varphi} = -\frac{1}{s_{44}\,x_n}\,\frac{\partial u_n}{\partial \varphi}, \tag{2.19}$$

$$\sigma_{n\theta} = -\frac{\Theta}{s_{44}\,x_n}\,\frac{\partial u_n}{\partial \nu}, \tag{2.20}$$

where Θ is given by Equation (1.13), and c_1, c_2, c_2 are derived as

$$c_1 = \frac{E}{(1+\mu)(1-2\mu)},\ c_2 = -\frac{\mu E}{(1+\mu)(1-2\mu)},\ c_3 = -4(1-\mu) < 0, \tag{2.21}$$

and $c_3 < 0$ due to $\mu < 0.5$ for real isotropic components (Skocovsky and Bokuvka and Palcek, 1996, 75-79).

If $a_{1i} = \cos[\angle(x_1,x_i)]$ $(i = n,\varphi,\theta)$ represent a direction cosine of an angle formed by axes x_1, x_i, then, with respect to Figures 1.4, 1.5, we get

$$\begin{aligned} &a_{1n} = \cos\varphi\,\sin\theta, \quad a_{1\varphi} = \sin\varphi\,\sin\theta, \quad a_{1\theta} = \cos\theta, \\ &a_{\varphi 1} = -\sin\varphi, \quad a_{\theta 1} = -\cos\varphi\cos\theta, \end{aligned} \tag{2.22}$$

where $\cos\theta$, $\sin\theta$ are given by Equation (1.12). The stress σ_1 along the axis x_1 has the form

$$\begin{aligned} \sigma_1 = {} & a_{1n}\,\sigma_n + a_{1\varphi}\,\sigma_\varphi + a_{1\theta}\,\sigma_\theta \\ & + a_{1n}(\sigma_{n\varphi} + \sigma_{n\theta}) + a_{1\varphi}\,\sigma_{\varphi n} + a_{1\theta}\,\sigma_{\theta n}. \end{aligned} \tag{2.23}$$

With regard to Equations (2.17)-(2.20) and due to $\sigma_{n\varphi} = \sigma_{\varphi n}$, $\sigma_{n\theta} = \sigma_{\theta n}$ (Brdicka, 2000, 65-67), we get